Interim Report
on the Study of

ELECTRODYNAMICS OF LONG CONDUCTING TETHERS IN THE NEAR-EARTH ENVIRONMENT

January 5, 1976

by
M. Dobrowolny
G. Colombo
M. D. Grossi

NASA Contract NAS8-31678

Smithsonian Institution
Astrophysical Observatory
Cambridge, Massachusetts 02138

ABSTRACT

An analytical approach has been developed to evaluate the electrodynamic interactions affecting a thin, bare metallic wire moving in the ionosphere. The wire's diameter is smaller than the Debye length; therefore, the plasma sheath around the wire must be taken into account in computing induction drag force and torque.

Computer programs have been prepared for the numerical evaluation of mathematical functions that are required to compute the distribution of the potential along the wire and of the current in the wire.

Numerical calculations based on this software are in progress.

FOREWORD

Although this report is not a contractual requirement, it was deemed appropriate to record the analytical developments to date. This should be useful for NASA-MSFC in reviewing SAO's progress and will serve SAO as a basis for detailed planning of the remainder of the program.

The 12 cases that are being investigated are shown in the matrix (Table I). We started with B.1.II (the long wire deployed in an electrodynamics-dominated environment) for several reasons. The most relevant is that it is probably the case that is closest to reality. That is, we expect that the configuration most likely to be used in Space Shuttle applications of the Skyhook concept is closely represented by case B.1.II. Furthermore, it is the case that centers upon pure electrodynamics, excluding the effects of atmospheric drag. Once this case is completed, it should not be overly difficult to extend the results analytically to a tether deployed in an environment dominated by atmospheric drag or to intermediate situations.

TABLE I

Study Structure - Tether Electrodynamics Investigation

Cases to be Investigated	Tether Deployed in Drag-Dominated Environment (I)	Tether Deployed in Electrodynamics-Dominated Environment (II)	Tether in Intermediate Situations (III)
A. Nonmetallic Tether			
B. Metallic Tether			
B.1 Noninsulated			
B.2 Insulated			
B.2.1 With terminating electrodes			
B.2.2 Without terminating electrodes			

We also continued the analysis of case B.2.1.II, which was initially examined by SAO as an in house effort and was illustrated in a presentation to NASA-MSFC that took place in the fall of 1974.

Still to be investigated are all cases A and B.2.2; we will leave them until last inasmuch as they are of less practical importance.

For case B.1.II we have developed the formalism required for computing the distribution of potential along the wire and the current in it, for both a perfect conductor and one with finite resistance. Computer programs have already been written for the numerical evaluation of the functions illustrated in Section A.1, A.2 and A.3 of Appendix A to this report. The next step will be the computation of the functions in A.4, following which will be the recomputation of all the above functions, taking into account the finite resistance of the wire. Finally, the functions in A.5 will be numerically evaluated, obtaining induction force and induction torque for case B.1.II, thus completing the case.

1. Introduction

In this report, we present and discuss a scheme for calculating electrodynamic forces acting on a long conducting wire in the ionospheric plasma. The essential part of this method is the determination of a convenient model that considers the sheath of charges surrounding a thin wire and the discussion of its validity. A short discussion is also given on how to take the effects of the wire's resistance into account.

Numerical work on the scheme presented is in progress.

2. Potential Distribution along the Wire

We refer to a wire of length L and radius r_w moving in the ionospheric plasma with a velocity V_0. The numbers to be given to these parameters are

$$L = 100\,km\,, \quad r_w = 0.15\,mm\,, \quad V_0 = 7\,km/sec \tag{1}$$

The top end of the wire will be considered to be at altitudes varying from 200 to 500 km.

As the wire moves in the earth's magnetic field $\underline{B}$, a $\underline{V}_0 \times \underline{B}$ electric field is set up on the wire. By referring to a perfectly conducting wire and to motion perpendicular to $\underline{B}$ lines, the potential at any point in the wire with respect to the plasma is given by

$$\varphi(z) = BV_0(z - z_0) \tag{2}$$

where z denotes the coordinate of a point in the wire with its z axis directed upward and its origin in the middle point of the wire (see Figure 1).

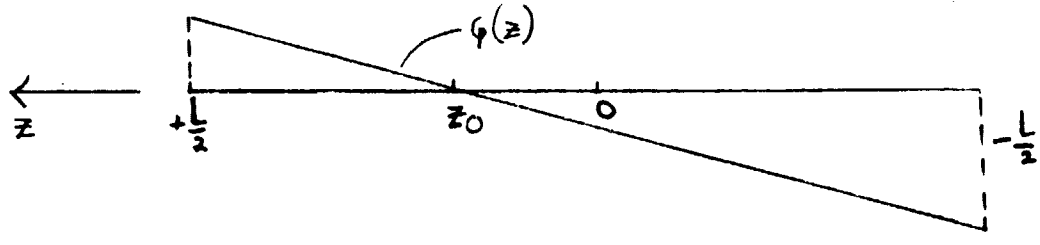

Figure 1. Coordinate system for the computation of potential distribution.

If we take B = 0.5 gauss for the magnetic field, the total potential drop along the length of the wire is

$$|\Delta V| = 35 \text{ kvolts}$$

The point z_0 of zero potential (wire at plasma potential) must be determined through a balance of all charged-particle fluxes to the wire,[1,2] i.e., by solving the equation

$$F(z_0) = 0 \tag{3}$$

where

$$F(z_0) = \int_{-\frac{L}{2}}^{+\frac{L}{2}} dz \left\{ f^{(i)}\left[\varphi(z, z_0)\right] - f^{(e)}\left[\varphi(z, z_0)\right] \right\} \tag{4}$$

and $f^{(j)}$ (j = 1, e for ions and electrons, respectively) represents the currents per unit length of particles of species j, depending on the potential distribution, equation (2).

In the following, photoelectron emission from the wire's surface will be neglected, and hence $f^{(j)}$ will represent just the particle flux collected by the wire from the surrounding plasma. From both experimental data and theoretical computations,[2] it does indeed appear that the photoelectron flux is negligible at the altitudes of interest, in comparison with particle fluxes from the plasma. In Ref. 2, where the photoelectron flux is taken into account, it is found that at 400 km, it is negligible compared to both electron and ion fluxes from the plasma. On the other hand, as will be seen, the particle fluxes computed in Ref. 2, where sheath effects were not taken into account (thin-sheath limit), are smaller than those expected in the thick-sheath case, which is the one of relevance to us. As a typical number to check a posteriori the consistency of the calculations that follow, we will refer to an average photoelectric current density,[3]

$$i_{ph} \sim 10^{-9} \text{ amp/cm}^2$$

3. Particle Fluxes Collected by the Wire

To calculate particle fluxes collected by the wire from the surrounding plasma, we must resort to the theory of plasma probes (see Ref. 4 for an up-to-date account on the state of the theory).

All the work that has been done on the probe theory refers to probes at constant potential (i.e., uniform over the probe's surface). In our case, we have a linear potential distribution on the wire (see eq. (2)). However, since the potential variation in the radial direction scales with the Debye length $\lambda_d = (KTe/4\pi ne^2)^{\frac{1}{2}}$, which is extremely small compared to the wire's length ($\lambda_d \simeq 0.2 \div 0.3$ cm between 100 and 400 km), the probe theory at constant potential can be applied locally at every point in the wire.

$$\frac{r_w}{\lambda_d} < 1 \qquad (5)$$

(for example, $r_w/\lambda_d = 7 \times 10^{-2}$ at 200 km); thus, the potential of the wire is expected to decrease over a long distance with respect to the wire's dimension. Neglecting the sheath around the wire, as in the calculations in Ref. 2, would then be completely inappropriate.

The probe theory is especially developed with reference to unmagnetized plasmas, whereas in the presence of a magnetic field, only particular cases can be treated.[4] In the cases of interest to us, the electron Larmor radius a_e is greater than the Debye length (a_e varies from 1.5 to 3.4 cm between 100 and 400 km), so that, in the region of potential variation around the wire, the effect of the magnetic field on particle orbits can be neglected; i.e., we can refer to the probe theory in the absence of magnetic fields.*

Under condition (5), the current collected by the probe can be computed, by using the terminology introduced in the early work of Langmuir and Mott-Smith,[5] in the "orbital motion limit" (OML) approximation. More precisely, the OML current is that current collected by the probe when none of the undisturbed plasma particles (at infinity) capable of reaching the probe on the basis of energy considerations is excluded from doing so by intervening

* This may not be justified for those regions of the wire where the surrounding sheath is especially thick (its thickness becoming comparable to or smaller than the electron Larmor radius). We can, however, predict that the main effect of the magnetic field for these circumstances is that of changing the effective cross section for electron collection (see Ref. 4) by a numerical factor (~2).

potential barriers. For attracted particles, this corresponds to an infinitely thick sheath, i.e., in fact, condition (5).

Assuming Maxwellian distributions for particles far from the collector and including the effect of plasma flow with respect to the probe (with velocity V_0), we obtain the following equation for the particle fluxes $f^{(j)}$ per unit length

$$f^{(j)}(\varphi) = \frac{\beta}{\sqrt{\pi}} r_w I_r^{(j)} e^{-\alpha_j^2} Y_j(\varphi) \tag{6}$$

where

$$\alpha_j = \frac{V_0}{V_{thj}} \tag{7}$$

$V_{thj} = (2KT_j/m_j)^{1/2}$ is the thermal velocity of j^{th} particles, and

$$I_r^{(j)} = N Z_j |e| V_{thj} \tag{8}$$

is the current density due to random thermal motion, N being the particle density ($N_i = N_e$ far from the probe), and $Z_e = 1$, $Z_i = 8$ (the main ion content at the altitudes considered is O^+). Finaliy, the dependence on the probe potential is contained in the following integrals:

$$Y_i = \int_0^{\pi} \int_{\sqrt{|\eta_i|},0}^{\infty} x \sqrt{x^2 \mp |\eta_i|}\, e^{-(x^2 - 2\alpha_i x \cos\theta)} dx d\theta \tag{9}$$

$$Y_e = \int_0^{\pi} \int_{0,\sqrt{|\eta|}}^{\infty} x \sqrt{x^2 \pm |\eta|}\, e^{-(x^2 - 2\alpha_e x \cos\theta)} dx d\theta \tag{10}$$

where the following notations have beenintroduced:

$$\eta = \frac{|e|\varphi}{KT_e} \quad , \quad \eta_i = \frac{Z_i |e| \varphi}{KT_i} \tag{11}$$

Furthermore, in both (9) and (10), the first or second lower limit of integration and, correspondingly, the upper or lower sign in the square root

under the integral are taken for positive ($\eta > 0$) or negative ($\eta < 0$) potentials, respectively.

It is useful to recall that a total particle current

$$I^{(j)} = 2\pi r_w L I_c^j \tag{12}$$

(of ions or electrons, according to the sign of the potential) would be collected by the wire in the opposite limit of a thin sheath (i.e., for $r_w > \lambda_d$). Whereas this current is independent of the potential, the OML current, given by formulas (6) to (10), depends on the potential and actually, for $\eta > 1$, is above the thin-sheath value, equation (12).

4. Comments on OML Formulas for Current Collection in the Wire

Several arguments will now be put forward to justify the use of the OML formulas for the current collected along the wire under consideration.

A first point is that, for the case of stationary plasmas, numerical solution of the full self-consistent problem of current collection by Laframboise,[6] involving the solution of Poisson's equation compled with the Vlasov equations for ion and electron distribution functions, reproduces the OML results, for the case of a cylindrical probe (for a large range of values of the probe's potential), in a domain of values of zw/λ_d, between zero and some finite value close to unity. For a stationary plasma ($\alpha_j = 0$ in our notation) and our values of r_w/λ_d, the OML formulas would therefore be completely accurate. Since the flow obviously influences particle collection, the effect of plasma flow with respect to the probe is, qualitatively, that of destroying the circular symmetry of the sheath around the cylinder; i.e., the potential field surrounding the cylinder becomes a function $\phi(r,\theta)$ where r and θ are polar coordinates in a plane perpendicular to the wire. In this case, the numerical solution of the self-consistent problem, which is quite prohibitive, is not available. However, studies of the problem under different approximations and from different points of view have been done,[6,7,8,9] so that a discussion on the validity of the OML formulas can still be made.

We know that the electron thermal velocity is considerably greater than the flow velocity V_0 for example,

$$\alpha_e = 3.9 \times 10^{-2} \tag{13}$$

at 200 km. As far as the electron contribution to the current $f^{(e)}$ is concerned, it is clear that the OML formulas (whose validity for $r_w/\lambda_d < 1$ is well checked in the stationary case) will give nearly correct results.

As far as the ions are concerned, thermal motion, on the contrary, is much slower than the directed motion,

$$\alpha_i \sim 9.5 \tag{14}$$

at 200 km. On physical grounds, we would say that around those regions of the wire of high potential where

$$|\eta| > \alpha_i^2$$

the collection is dominated by electrostatic forces (the electrical voltage is much greater than the voltage equivalent of the ion drift velocity V_0) and therefore the OML formulas should be accurate. On the other hand, for regions of the wire at very small potential, namely, where

$$|\eta| \ll \alpha_i^2$$

as shown by Langmuir and Mott-Smith,[5] the OML formulas (6) to (10) give, for the ion current,

$$-I^{(i)} \sim 2\pi r_w N|e|V_0\sqrt{1 - \frac{\eta_i}{\alpha_i^2}}$$

which is what is obtained by considering a unidirectional stream of ions of equal velocity (and hence a physically correct limit, since, for these small potentials, collection is dominated by the ion drift). Hence, from physical arguments, it is seen that it is only for the points of the wire where

$$|\eta| \sim \alpha_i^2$$

that the OML formulas could be more inaccurate. As integrals must be done over the wire's length (both for the calculation of the potential distribution on the wire, see eq. (4), and for the successive calculation of current distribution, see Section 5), we expect the OML formulas, including the effect of velocity flow, also to be sufficiently good for ion collection.

Further strength on this conclusion is obtained from the work of Smetana[9] on currents collected by a cylinder in a rarefied plasma flow. Here the author derives OML currents, assuming a circularly symmetric sheath around the cylinder, but keeps as a parameter in his formulas the sheath radius d* ($d - r_w$ being the distance in which the potential drop between the probe and the plasma is assumed to occur). Our formulas (6) to (10) correspond to the limit $d/r_w \to \infty$ in his formulas, in which the dependence on d disappears. By varying the parameter d/r_w, Smetana then investigates numerically the current collection by the cylinder as a function of the potential η. His results, corresponding to values of α_i around the value of interest to us, equation (14), show only very slight variations with d/r_w (compare, for example, the curves in his Fig. 2a-2c corresponding to $d/r_w = 1$ and $d/r_w = 100$), with a tendency for the currents obtained with $d/r_w \gg 1$ to be slightly larger than those for small d/r_w at high potential values ($\eta \gg 1$).

The main conclusion of this work is that the actual sheath dimensions can, at most, imply an error of 5 to 10% with respect to the value obtained in the infinite sheath limit for particular (and high) potential values.

5. Current Distribution along the Wire and Electromagnetic Drag Forces

Once we have determined the point on the wire at plasma potential (z_0), and hence the potential distribution along the wire, we can calculate the current distribution on the wire. Taking into account the electron current (from the negative to the positive end of the wire), the magnitude at any point z will be found from

$$I(z) = \int_{-\frac{L}{2}}^{z} \left\{ f^{(e)}\left[\varphi(z')\right] - f^{(i)}\left[\varphi(z')\right] \right\} dz' \qquad (15)$$

where the functions $f^{(j)}$ were defined in Section 3. Notice that the maximum of the current profile (15) corresponds to the point z_0 of zero potential on the wire. In fact, we see that it is at $z = z_0$ that the imbalance between ion and electron fluxes is maximum.

---

* The value of d can, of course, be determined only through the solution of Poisson's equation with self-consistent particle densities.

The electromagnetic forces on the wire due to the current induced by the $\underline{V}_0 \times \underline{B}$ effect are then computed from the appropriate moments of the current distribution, equation (15).

The induction drag $\underline{F}_D$ will thus be given by the sum of the $\underline{I} \times \underline{B}$ forces everywhere on the wire, i.e.,

$$F_D = B \int_{-\frac{L}{2}}^{+\frac{L}{2}} I(z)\, dz \tag{16}$$

where the earth's magnetic field $\underline{B}$ can be considered constant along the length of the wire.

The induction torque T about the wire's center is found from

$$T = B \int_{-\frac{L}{2}}^{+\frac{L}{2}} z\, I(z)\, dz \tag{17}$$

6. Effect of the Wire's Internal Resistance

In this section, we briefly comment on the effects of the wire's internal resistance on the potential and current distribution along the wire.

The wire crossing the earth's magnetic-field lines constitutes a DC generator. By referring to an element dz of the wire, between coordinates z and z + dz, Ohm's law can be written

$$i(z)\, dR + d\phi(z) = V_0 B\, dz \tag{18}$$

where i(z) is the current at the given element, dR is its resistance and $d\phi(z) = \phi(z+dz) - \phi(z)$ is the potential difference across the element. If all the wire is made of the same material, and is of the same cross section, we have

$$dR = \frac{R}{L}\, dz \tag{19}$$

where R is the total wire resistance. For a steel wire (resistivity $\rho = 0.15\ \mu\Omega m$) of length 100 km and radius $r_w = 0.15$ mm, we have R = 212 kΩ.

Integrating equation (18) from one end (-L/2) of the wire to any given point z, we obtain

$$\frac{\rho}{L}\int_{-\frac{L}{2}}^{z} i(z')dz' + \Delta\phi_1(z) = V_0 B\left(z+\frac{L}{2}\right) \qquad (20)$$

with

$$\Delta\phi_1(z) = \phi_1(z) - \phi_1\left(-\frac{L}{2}\right) \qquad (21)$$

Neglecting the wire's resistance, we have

$$\Delta\phi_1(z) = V_0 B\left(z+\frac{L}{2}\right) = \Delta\phi_0(z) \qquad (22)$$

i.e., the linear potential distribution, equation (2).

Ohm's law, equation (20), therefore shows that the wire's resistance will lower the potential difference between points of the wire with respect to the value corresponding to $\Delta\phi_0(z)$.

Since the potential distribution along the wire is needed to calculate the particle currents collected by the plasma, according to the scheme of Sections 3 and 4, we must conclude that equation (20), where $\Delta\phi(z)$ depends on the current distribution i(z), cannot be used directly.

A method of using equation (20) in an iteration scheme, ending up with a full account of the wire's actual resistance, is currently under study.

7. Forthcoming Developments in This Study

Forthcoming developments in this study will first of all consist of the derivation of numerical results for the current and potential distributions along the wire (case B.1.II) according to the scheme and formulas given herein. Ionospheric models for charged-particle density and temperature as a function of altitude will be used in these calculations.

This will lead to accurate values for the total induction drag and torque at various altitudes for the wire, to be compared with corresponding values of aerodynamic drag.

Knowledge of the potential distribution along the wire (taking into account the effects of the wire's resistance) is also preliminary to the study of Coulomb drag forces on the wire. This knowledge will, in fact, allow a model to be made of the charged sheath surrounding the object, and therefore it will be possible to calculate electrostatic-drag contributions.

8. References

1) D. B. Beard and F. S. Johnson, "Charge and magnetic field interaction with satellites." Journ. Geophys. Res., vol. 65, p. 1, 1960.

2) C. K. Chu and R. A. Cross, "Alfvèn waves and induction drag on long cylindrical satellites." AIAA Journ., vol. 4, p. 2209, 1966.

3) M. A. Kasha, The Ionosphere and Its Interaction with Satellites. Gordon and Breach, Science Publ., New York, 1969.

4) P. M. Chung, L. Talbot, and K. J. Touryan, Electric Probes in Stationary and Flowing Plasmas: Theory and Application. Springer-Verlag, 1975.

5) I. Langmuir and H. M. Mott-Smith, "The theory of collections in gaseous discharges." Phys. Rev., vol. 28, p. 727, 1926.

6) J. G. Laframboise, "Theory of spherical and cylindrical Langmuir probes in a collisionless maxwellian plasma at rest." UTIAS Report, no. 100, University of Toronto, 1966.

7) R. T. Bettingen and A. A. Chou, "An end effect associated with cylindrical Langmuir probes moving at satellite velocities." Journ. Geophys. Res., vol. 73, p. 2513, 1968.

8) J. R. Sanmartin, "End effect in Langmuir probe response under ionospheric satellite conditions." Phys. Fluids, vol. 15, p. 1134, 1972.

9) F. O. Smetana, "On the current collected by a charged circular cylinder immersed in a two dimensional rarefied plasma stream." In Rarefied Fluid Dynamics, ed. by J. A. Laurmann, Vol. II, p. 65, 1963.

APPENDIX A

SUMMARY OF COMPUTATIONAL STEPS FOR CASE B.1.II

A.1 Input definitions and parameter values

$$B(\zeta) = 5 \times 10^{-5}$$

$$V_0 = 7 \times 10^3$$

$$L = 10^5$$

$$T_e(\zeta) = 0.154$$

$$T_i(\zeta) = \frac{1}{2} T_e(\zeta)$$

$$z_w = 1.5 \times 10^{-4}$$

$$N(\zeta) = 6.728 \times 10^{11}$$

$$Z_i = 8$$

$$Z_2 = 1$$

$$v_{thi} = 1.38 \times 10^4 \frac{1}{\sqrt{2 Z_i}} \sqrt{T_i(\zeta)}$$

$$v_{the} = 5.95 \times 10^5 \sqrt{T_e(\zeta)}$$

$$\eta_i = Z_i \cdot \frac{T_e(\zeta)}{T_i(\zeta)} \eta$$

$$|e| = 1.602 \times 10^{-19}$$

$$\chi(\zeta) = 1.902 \cdot 10^5$$

A:2 Determine the zero of the following function

$$F(\zeta_0) = \int_{-\frac{1}{2}}^{+\frac{1}{2}} d\zeta \left\{ f^{(i)}\left[\eta(\zeta,\zeta_0)\right] - \left| f^{(2)}\left[\eta(\zeta,\zeta_0)\right] \right| \right\}$$

where

$$\eta(\zeta,\zeta_0) = \chi(\zeta)(\zeta - \zeta_0)$$

$$\chi(\zeta) = \frac{|z| B(\zeta) V_0 L}{T_e(\zeta)}$$

$$f^{(i)}\left[\eta(\zeta,\zeta_0)\right] = \frac{8}{\sqrt{\pi}} \pi_w I_R^{(i)} e^{-\alpha_j^2} Y_j\left[\eta(\zeta,\zeta_0)\right]$$

$$I_R^{(i)} = N(\zeta) Z_j |z| V_{Tj}$$

$$\alpha_j = \frac{V_0}{V_{Thj}}$$

ζ_0 can be varied between $+\frac{1}{2}$ and $-\frac{1}{2}$ the zero should probably be around the

values

A.3 Checks on the numerical computations of the Y_j integrals

A.3.1 Computing the integrals $Y_2^{(\pm)}$ for $\alpha_2 = 0$, one should find

$$Y_2^{(+)}(\alpha_2=0) = \frac{\pi}{2}\left[\sqrt{\eta} + \frac{\sqrt{\pi}}{2} e^{\eta}\left(1 - \mathrm{erf}\sqrt{\eta}\right)\right] \qquad (\eta>0)$$

$$Y_2^{(-)}(\alpha_2=0) = \frac{\pi^{3/2}}{4} e^{-|\eta|} \qquad (\eta<0)$$

with $\mathrm{erf}(x) = \frac{2}{\sqrt{\pi}} \int_0^x d\xi\, e^{-\xi^2}$

A.3.2 The result of the integral $Y_i^{(+)}$ should be compared with the following Bessel function series

$$Y_i^{(+)} = \frac{\pi^{3/2}}{4} e^{\eta_i} \sum_{p=0}^{\infty} \frac{(2p-1)!}{2^{2p}(p!)^2} \left(\frac{\alpha_i}{\sqrt{\eta_i}}\right)^p i^{-p} J_p\left(2\alpha_i i\sqrt{\eta_i}\right)$$

A.3.3 The results of the integrals $Y_i^{(\pm)}$ for values of η such that

$$|\eta_i| \ll \alpha_i^2$$

A.4 Calculation of the current distribution

Compute the following function of ς

$$I(\varsigma) = L \int_{\varsigma}^{\frac{1}{2}} d\varsigma' \left\{ \left| f^{(2)}[\eta(\varsigma')] \right| - f^{(i)}[\eta(\varsigma')] \right\}$$

where the function $f^{(i)}$ are defined at § II and III,

$$\eta(\varsigma') = \chi(\varsigma')(\varsigma' - \varsigma_0^*)$$

and ς_0^* is the zero of the function $F(\varsigma_0)$ found in A.2, i.e.

$$F(\varsigma_0 = \varsigma_0^*) = 0$$

The variable ς must be varied in the interval

$$-\frac{1}{2} \leq \varsigma \leq \frac{1}{2}$$

A.5 Calculation of induction drag and torque

Compute the following quantities:

$$D = L \int_{-\frac{1}{2}}^{+\frac{1}{2}} B(\zeta) I(\zeta) d\zeta$$

$$M = L \int_{-\frac{1}{2}}^{+\frac{1}{2}} \zeta B(\zeta) I(\zeta) d\zeta$$